Acta Crystallographica Section D
Biological Crystallography
ISSN 1399-0047

Structure of ADC-68, a novel carbapenem-hydrolyzing class C extended-spectrum β-lactamase isolated from *Acinetobacter baumannii*

Jeong Ho Jeon,[a]‡ Myoung-Ki Hong,[b,c]‡ Jung Hun Lee,[a]‡ Jae Jin Lee,[a] Kwang Seung Park,[a] Asad Mustafa Karim,[a] Jeong Yeon Jo,[a] Ji Hwan Kim,[a] Kwan Soo Ko,[d] Lin-Woo Kang[b,c]* and Sang Hee Lee[a]*

[a]National Leading Research Laboratory of Drug Resistance Proteomics, Department of Biological Sciences, Myongji University, 116 Myongjiro, Yongin, Gyeonggido 449-728, Republic of Korea, [b]Institute for Cellular and Structural Biology of Sun Yat-Sen University, Guangzhou, Peoples Republic of China, [c]Department of Biological Sciences, Konkuk University, Hwayang-dong, Gwangjin-gu, Seoul 143-701, Republic of Korea, and [d]Department of Molecular Cell Biology, Samsung Biomedical Research Institute, Sungkyunkwan University School of Medicine, Suwon, Republic of Korea

‡ These authors contributed equally to this paper.

Correspondence e-mail: lkang@konkuk.ac.kr, sangheelee@mju.ac.kr

Received 2 July 2014
Accepted 28 August 2014

PDB reference: ADC-68, 4qd4

Outbreaks of multidrug-resistant bacterial infections have become more frequent worldwide owing to the emergence of several different classes of β-lactamases. In this study, the molecular, biochemical and structural characteristics of an *Acinetobacter*-derived cephalosporinase (ADC)-type class C β-lactamase, ADC-68, isolated from the carbapenem-resistant *A. baumannii* D015 were investigated. The $bla_{\text{ADC-68}}$ gene which encodes ADC-68 was confirmed to exist on the chromosome *via* Southern blot analysis and draft genome sequencing. The catalytic kinetics of β-lactams and their MICs (minimum inhibitory concentrations) for *A. baumannii* D015 and purified ADC-68 (a carbapenemase obtained from this strain) were assessed: the strain was resistant to penicillins, narrow-spectrum and extended-spectrum cephalosporins, and carbapenems, which were hydrolyzed by ADC-68. The crystal structure of ADC-68 was determined at a resolution of 1.8 Å. The structure of ADC-68 was compared with that of ADC-1 (a non-carbapenemase); differences were found in the central part of the Ω-loop and the C-loop constituting the edge of the R1 and R2 subsites and are close to the catalytic serine residue Ser66. The ADC-68 C-loop was stabilized in the open conformation of the upper R2 subsite and could better accommodate carbapenems with larger R_2 side chains. Furthermore, a wide-open conformation of the R2-loop allowed ADC-68 to bind to and hydrolyze extended-spectrum cephalosporins. Therefore, ADC-68 had enhanced catalytic efficiency against these clinically important β-lactams (extended-spectrum cephalosporins and carbapenems). ADC-68 is the first reported enzyme among the chromosomal class C β-lactamases to possess class C extended-spectrum β-lactamase and carbapenemase activities.

1. Introduction

Acinetobacter baumannii is increasingly being recognized as a crucial pathogen that is associated with nosocomial infections and is frequently involved in infectious outbreaks in intensive care units and burns units (Bergogne-Bérézin & Towner, 1996; Poirel & Nordmann, 2006). Multidrug-resistant isolates of *A. baumannii* have frequently been reported during the last decade, and carbapenem resistance in this species has recently been increasing worldwide (Coelho *et al.*, 2004; Richet *et al.*, 2001). Since carbapenems are used to effectively treat *Acinetobacter* infections, the emergence of carbapenem-resistant *A. baumannii* strains has created substantial therapeutic challenges (Coelho *et al.*, 2004).

Recent phylogenetic analyses have revealed that the chromosomal AmpC (class C β-lactamase) genes in *Acinetobacter* spp. probably descended from a single common β-lactamase (*bla*) gene ancestor. The chromosomal AmpC genes in

Acinetobacter spp. are designated as *Acinetobacter*-derived cephalosporinases (ADCs; Hujer *et al.*, 2005; Perez *et al.*, 2007). ADCs can hydrolyze cephalosporins such as cefotaxime and ceftazidime but not cefepime or carbapenems. Two ADC derivatives, ADC-33 and ADC-56, have recently been reported to be able to hydrolyze cefepime (Rodríguez-Martínez *et al.*, 2010; Tian *et al.*, 2011). However, until recently no ADC enzymes had been shown to display carbapenem-hydrolyzing activity.

Extended-spectrum β-lactamases (ESBLs) are defined as β-lactamases that are able to hydrolyze penicillins, narrow-spectrum cephalosporins (cephalothin), extended-spectrum cephalosporins (cefotaxime and ceftazidime) and monobactams (aztreonam) but not cephamycins or carbapenems (Paterson & Bonomo, 2005). According to recent ESBL definitions, the ESBLs have been divided into class A ESBLs (aESBLs), class C ESBLs (cESBLs) and class D ESBLs (dESBLs) (Lee *et al.*, 2009, 2012).

Extended-spectrum class C (AmpC) β-lactamases are designated as cESBLs. Most cESBLs that are produced by Gram-negative pathogens isolated from clinical specimens from patients have extended their substrate specificity to narrow-spectrum and extended-spectrum cephalosporins (Lee *et al.*, 2009, 2012). The extended substrate spectrum of cESBLs has been demonstrated by the crystallographic structures of GC1 and CMY-10 (Crichlow *et al.*, 1999; Kim *et al.*, 2006). Kinetic data, MIC values and the crystal structure revealed that GC1 is a natural cESBL owing to the flexibility of the Ω-loop caused by the insertion of Ala-Val-Arg after position 210 compared with P99 from *Enterobacter cloacae* P99, which is a class C β-lactamase and a non-ESBL (Crichlow *et al.*, 1999; Nukaga *et al.*, 1995). Crystallographic and biochemical research on the CMY-10 enzyme demonstrated that a three-amino-acid deletion in the R2-loop of CMY-10 appears to be responsible for the extended-spectrum activity of CMY-10 and that this deletion significantly widens the R2 subsite, which accommodates the R_2 side chains of β-lactams (Kim *et al.*, 2006).

Carbapenemases are the most versatile family of β-lactamases and are able to hydrolyze carbapenems and other β-lactams (Queenan & Bush, 2007). Carbapenems (imipenem, meropenem and ertapenem) have the broadest spectra of antimicrobial activity among all β-lactams and are primarily used to treat infections by aerobic Gram-negative bacteria. According to their dependency on divalent cations for enzyme activation, carbapenemases can be divided into metallo-carbapenemases (zinc-dependent class B) and non-metallo-carbapenemases (zinc-independent classes A, C and D) (Lee & Lee, 2006).

Class A carbapenemases, which include the KPC, IMI, SME and NMC-A families and some GES enzymes, have most frequently been discovered in isolates from Enterobacteriaceae and in species such as *Pseudomonas aeruginosa* (Lee & Lee, 2006; Thomson, 2010). These enzymes are inhibited by clavulanate, except for some KPC-type enzyme(s) such as KPC-2, and hydrolyze penicillins or cephalosporins more efficiently than carbapenems. Class B carbapenemases, which include the VIM and IMP families as well as SPM-1, have previously been detected in strains of *Pseudomonas aeruginosa*, members of the Enterobacteriaceae family and *A. baumannii* (Thomson, 2010). These carbapenemases hydrolyze penicillins, cephalosporins and carbapenems; however, they lack the ability to hydrolyze aztreonam. Class D carbapenemases belong to the OXA family and were identified in *Acinetobacter* clinical isolates (Afzal-Shah & Livermore, 1998); they weakly hydrolyze carbapenems and are poorly inhibited by clavulanate (Thomson, 2010).

Recently, class C carbapenemases that can hydrolyze carbapenems, including CMY-2, ACT-1 and DHA-1, have been identified in Enterobacteriaceae (Kim *et al.*, 2006; Mammeri *et al.*, 2010; Lee *et al.*, 2007; Bradford *et al.*, 1997). These carbapenemases are plasmid-mediated class C β-lactamases that exhibit catalytic activity for imipenem (Mammeri *et al.*, 2010). In addition, CMY-10 revealed catalytic activity for imipenem (Kim *et al.*, 2006).

A modelling study of CMY-2 and ACT-1 revealed that their large R2 subsites might improve their accommodation of imipenem inside the catalytic pocket (Mammeri *et al.*, 2010). This indicates that structural differences in the R2 subsite may have an effect on carbapenem hydrolytic activity. In this study, we report the molecular, biochemical and structural characterization of ADC-68, which is a class C extended-spectrum β-lactamase (cESBL) and carbapenemase from *A. baumannii* D015.

2. Materials and methods

2.1. Bacterial isolates and strains

A total of 48 clinical isolates of carbapenem-resistant *A. baumannii* were collected from the blood of various patients from five tertiary-care hospitals in Korea from 2002 to 2006. The strains and plasmids used in this study are listed in Supplementary Table S1[1]. *Escherichia coli* ATCC 25922, *E. coli* TOP10, *E. coli* BL21(DE3) and plasmid-containing *E. coli* strains were grown in Luria–Bertani (LB) medium (Difco Laboratories, Detroit, Michigan, USA) at 37°C. The media were solidified with 1.8%(*w*/*v*) agar as necessary. Antibiotics were added as required to the following final concentrations: kanamycin, 50 mg l^{-1}; chloramphenicol, 25 mg l^{-1}.

2.2. Antimicrobial susceptibility tests

Susceptibility to ampicillin, piperacillin, amoxicillin, cephalothin, cefotaxime, ceftazidime, imipenem, meropenem (Sigma Chemical Co., St Louis, Missouri, USA) and ertapenem (MSD, Munich, Germany) was determined by an agar-dilution technique in Mueller–Hinton agar (Difco Laboratories, Detroit, Michigan, USA) with an inoculum of 10^4 CFU per spot. The results were interpreted according to the CLSI guidelines (Clinical and Laboratory Standards Institute, 2014).

[1] Supporting information has been deposited in the IUCr electronic archive (Reference: DW5111).

2.3. Identification and cloning of the bla_{ADC-68} gene

The primers used in this study are listed in Supplementary Table S1. The primer pair ABAMPC-1 and ABAMPC-2 was used for PCR amplification and identification of the ADC-type gene of *Acinetobacter* sp. (Bou & Martínez-Beltrán, 2000). Total DNA was extracted from *A. baumannii* D015 with a DNeasy Blood & Tissue Kit (Qiagen, Valencia, California, USA). The bla_{ADC-68} gene (the *bla* gene that codes for the 1152 bp ADC-68) from *A. baumannii* D015 was cloned after PCR amplification with the same primer pair (ABAMPC-1 and ABAMPC-2) and then sequenced.

To determine the minimum inhibitory concentrations (MICs) of ADC-68-producing strains, the bla_{ADC-68} gene was obtained by PCR using the primer pair *Sac*I-ADC-68 and *Xba*I-ADC-68 and the chromosomal DNA template from *A. baumannii* D015. The PCR products were electrophoresed in 1% agarose gels with TAE, removed from the gel using a QIAquick Gel Extraction kit (Qiagen, Valencia, California, USA) and the purified DNA was double-digested with *Sac*I and *Xba*I. The digested DNA was then cloned into the pHSG398 vector (Takara, Kusatsu, Japan) which was digested with the same DNA restriction enzymes to produce the pHSG398/bla_{ADC-68} plasmid. After verifying the DNA sequence, the recombinant plasmid was transformed into *E. coli* TOP10.

To express bla_{ADC-68} without the putative sequence of the signal peptide (Beceiro *et al.*, 2004), this gene was amplified by PCR using the primer pair *Nco*I-EK-HIS-ADC-68-F and *Xho*I-ADC-68-R. The amplified DNA and pET-28a(+) vector were double-digested with *Nco*I and *Xho*I, and the digested DNA was then cloned into the digested pET-28a(+) vector (Novagen, Madison, Wisconsin, USA) to produce the pET-28a(+)/His_6-bla_{ADC-68} plasmid. After verifying the DNA sequence, the recombinant plasmid was transformed into *E. coli* BL21 (DE3).

2.4. Pulsed-field gel electrophoresis (PFGE) and Southern blot analysis

The cells were grown overnight at 37°C in LB broth with appropriate antibiotics, diluted tenfold in fresh LB broth and shaken for 3 h. The cells were embedded in low-melting-point agarose with a contour-clamped homogeneous electric field (CHEF) Mapper XA system 50-well plug mould (Bio-Rad, Hercules, California, USA) according to the manufacturer's instructions and were modified as described previously (Barton *et al.*, 1995). An agarose block containing lysozyme- and protease K-treated cells was maintained in storage buffer at 4°C. The plug was extensively washed with TE and treated with 100 U of the enzyme I-*Ceu*I (New England Biolabs, Beverly, Massachusetts, USA) in 100 µl 1× digestion buffer to linearize the genomic DNA by cutting the prokaryotic 23S rRNA gene (Liu *et al.*, 1993). The plug was embedded in a CHEF gel (1%) and the bacterial DNA was electrophoresed using a CHEF-DRII system (Bio-Rad, Hercules, California, USA) at 14°C. Pulse times were ramped from 50 to 90 s over 22 h in 0.5× TBE (as running buffer) at 6 V cm^{-1}.

The gels were stained with ethidium bromide and observed on a UV transilluminator. The genome fragments were transferred onto a positively charged nylon membrane (Roche Diagnostics, Indianapolis, Indiana, USA). The membrane-bound fragments were UV cross-linked and hybridized with a PCR-generated probe that is specific for the 16S rRNA, bla_{ADC-68} or bla_{AmpC} gene using the associated primer pairs (Supplementary Table S1; Yakupogullari *et al.*, 2008). Labelling and detection were performed with a digoxigenin (DIG) DNA labelling and detection kit according to the manufacturer's instructions (Roche Diagnostics, Indianapolis, Indiana, USA).

2.5. Draft genome sequence and annotation analysis of *A. baumannii* D015

The genomic DNA of *A. baumannii* D015 was sequenced using an Illumina_Miseq_PE_250 system (5 981 754 reads; 333.49-fold coverage). Genome assembly was achieved using *Newbler assembler* 2.6 (Roche Diagnostics, Indianapolis, Indiana, USA), *CLC Genomics Workbench* 6.0 (CLC bio, Aarhus, Denmark) and *CodonCode Aligner* (CodonCode Corporation, Dedham, Massachusetts, USA). Gene prediction was carried out using *GLIMMER* 3 (Delcher *et al.*, 2007) and gene annotation was performed using the Clusters of Orthologous Groups (COG) and SEED databases (Disz *et al.*, 2010; Tatusov *et al.*, 1997). Database similarity was determined by a *BLAST* search (http://www.ncbi.nlm.nih.gov). Multiple alignments of nucleotide sequences between the *folE* and bla_{AmpC} genes of six *A. baumannii* strains were performed with *ClustalW* (http://align.genome.jp).

2.6. Expression and purification of ADC-68

The transformed cells were grown in LB medium (Difco Laboratories, Detroit, Michigan, USA) containing 50 mg l^{-1} kanamycin at an $OD_{600\,nm}$ of 0.6 at 37°C, and ADC-68 expression was induced with 0.5 m*M* isopropyl β-D-1-thio-galactopyranoside (IPTG) for 16 h at 30°C. The cells were harvested by centrifugation at 5000*g* for 30 min at 4°C, resuspended in 10 m*M* 2-(*N*-morpholino)ethanesulfonic acid (MES) buffer pH 6.8 and then disrupted by sonication. The crude lysate was then centrifuged at 20 000*g* for 30 min at 4°C and the clarified supernatant was loaded onto a His-Bind column (Novagen, Wisconsin, Wisconsin, USA) that was equilibrated with binding buffer (20 m*M* sodium phosphate pH 7.9, 10 m*M* imidazole, 500 m*M* NaCl). His_6-EK-ADC-68 was eluted with the same buffer but containing 500 m*M* imidazole.

For further purification, the His_6 tag was removed from His_6-EK-ADC-68 using enterokinase according to the manufacturer's instructions (Novagen, Madison, Wisconsin, USA). The reaction mixture was desalted and concentrated using a Fast Desalting column (Amersham Biosciences, Little Chalfont, England) and then loaded onto a Mono S column (Amersham Biosciences, Little Chalfont, England) that was pre-equilibrated with 10 m*M* MES pH 6.8. ADC-68 was eluted with a linear gradient from 0 to 0.5 *M* NaCl in MES buffer.

Table 1
Data-collection and refinement statistics.

Values in parentheses are for the highest resolution shell.

Data collection	
X-ray source	5C, PLS
Space group	$P2_12_12_1$
Unit-cell parameters (Å, °)	a = 56.4, b = 71.0, c = 179.5, $\alpha = \beta = \gamma$ = 90.0
Resolution (Å)	50.00–1.80 (1.86–1.80)
Total reflections	275071
Unique reflections	65468
Completeness (%)	96.2 (90.7)
Multiplicity	4.2 (4.2)
$\langle I/\sigma(I)\rangle$	29.0 (4.5)
R_{merge} (%)	7.1 (38.8)
Refinement	
Resolution (Å)	35.50–1.80
No. of reflections	62076
R_{work}/R_{free} (%)	18.8/23.6
No. of atoms	
Protein	5680
Ligand	
Citrate	26
MES	24
Water	430
B factors (Å^2)	
Protein	25.4
Ligand	
Citrate	32.1
MES	30.9
Water	31.3
R.m.s. deviations	
Bond lengths (Å)	0.020
Bond angles (°)	1.982
Ramachandran plot (%)	
Favoured	95.8
Allowed	3.8
Disallowed	0.4
PDB code	4qd4

The soluble form of ADC-68 without the His_6 tag was obtained with a yield of 9.8 mg of homogeneous protein per litre of culture. The purified ADC-68 was dialyzed against 10 mM MES buffer pH 6.8 and subsequently concentrated to 18.3 mg ml^{-1} for crystallization trials. Like other class C β-lactamases, the apparent molecular weight of the purified ADC-68 was estimated to be 40.5 kDa by SDS–PAGE.

2.7. Isoelectric focusing

Isoelectric focusing (IEF) was carried out in a Ready Gel Precast IEF polyacrylamide gel containing Ampholine (pH range 3–10) in a Mini-Protein 3 cell according to the manufacturer's instructions (Bio-Rad, Hercules, California, USA). The gels were developed with 0.5 mM nitrocefin (Oxoid, Basingstoke, England; Walsh *et al.*, 1996).

2.8. Steady-state kinetics analysis

Kinetic assays were conducted at 30°C with a Shimazu UV-1650PC spectrophotometer. Hydrolysis of β-lactams was detected by monitoring the variation in absorbance using the characteristic molecular extinction coefficient of each substrate: benzylpenicillin ($\Delta\varepsilon_{233}$ = −780 M^{-1} cm^{-1}), ampicillin ($\Delta\varepsilon_{235}$ = −900 M^{-1} cm^{-1}), piperacillin ($\Delta\varepsilon_{235}$ = −793 M^{-1} cm^{-1}), cephalothin ($\Delta\varepsilon_{262}$ = −7660 M^{-1} cm^{-1}), cefotaxime ($\Delta\varepsilon_{264}$ = −7250 M^{-1} cm^{-1}), ceftazidime ($\Delta\varepsilon_{265}$ = −10 300 M^{-1} cm^{-1}), imipenem ($\Delta\varepsilon_{278}$ = −5660 M^{-1} cm^{-1}), meropenem ($\Delta\varepsilon_{298}$ = −9530 M^{-1} cm^{-1}) and ertapenem ($\Delta\varepsilon_{295}$ = −10 940 M^{-1} cm^{-1}).

The assays were conducted in 10 mM MES buffer pH 6.8 containing enzymes (0.05–0.3 nM), substrates (10–500 µM) and bovine serum albumin (20 µg ml^{-1}). Steady-state kinetic constants were determined by fitting the initial rates (in triplicate) directly to the Henri–Michaelis–Menten equation using nonlinear regression with the program *DynaFit* (Kuzmic, 1996). When the K_m values were two low to be determined, the values were determined as competitive inhibition constants, K_i, in the presence of a good reporter substrate (100 µM cephalothin) and K_i values were calculated as described previously (Galleni & Frère, 1988; De Meester *et al.*, 1987; Galleni *et al.*, 1994).

2.9. IC_{50} determination

Inhibition of enzyme activity was determined under the same conditions with 100 µM cephalothin as the reporter substrate after a 5 or 10 min pre-incubation of 3 nM ADC-68 with various concentrations of inhibitors. IC_{50} corresponded to the inhibitor concentration needed to reduce the initial rate of hydrolysis of cephalothin by 50%.

2.10. Crystallization, data collection and structure determination

Crystallization conditions were screened using the sitting-drop vapour-diffusion method with a Hydra II eDrop automated pipetting system (Matrix Technologies Ltd, Stafford, England) at 14°C. The drops consisted of 0.5 µl protein solution (5 mg ml^{-1} in 10 mM MES pH 6.8) and 0.5 µl reservoir solution and were equilibrated against 70 µl reservoir solution at 14°C. The initial crystallization conditions tested were from the Morpheus kit (Molecular Dimensions, Suffolk, England). After one week, crystals were observed using Morpheus condition No. 2-25 (0.1 M carboxylic acids, 0.1 M buffer system 1 pH 6.5, 30% P550MME_P20K). The reservoir solution itself was used as a cryoprotectant solution. The crystal was mounted in a loop and transferred to the reservoir solution for 1 min prior to cooling in liquid nitrogen. The cryoprotected crystal was then mounted on the goniometer in a stream of cold nitrogen at −173°C.

X-ray diffraction data were collected at −173°C using an ADSC Q315r detector on beamline 5C SB II at Pohang Light Source (PLS), Republic of Korea, which is a synchrotron-radiation source. X-ray diffraction data were collected to 1.8 Å resolution from the ADC-68 crystal. The diffraction data were integrated and scaled *via* the *DENZO* and *SCALEPACK* crystallographic data-reduction routines (Otwinowski & Minor, 1997). The crystals belonged to the orthorhombic space group $P2_12_12_1$ with unit-cell parameters a = 56.4, b = 71.0, c = 179.5 Å. Matthews coefficient analysis indicated that two molecules may be present in the asymmetric unit, with a corresponding V_M of 2.22 Å^3 Da^{-1} and a solvent content of 44.6%.

The structure was determined by the molecular-replacement method using *MOLREP* (Vagin & Teplyakov, 2010) with the class C β-lactamase CMY-10 from *Enterobacter aerogenes* (PDB entry 1zkj, 43.7% sequence identity; Kim *et al.*, 2006) as a search model. The models were further built manually using *Coot* (Emsley *et al.*, 2010) and were refined using *REFMAC*5 (Murshudov *et al.*, 2011). The data-collection and refinement statistics are provided in Table 1. Structural figures were prepared using *PyMOL* (DeLano, 2002).

2.11. Accession numbers of the protein structure and the region surrounding the *bla*$_{\text{ADC-68}}$ gene

The coordinates and structure factors of ADC-68 have been deposited in the Protein Data Bank as entry 4qd4. The nucleotide sequence of the *bla*$_{\text{AmpC}}$ gene and the region surrounding the *bla*$_{\text{ADC-68}}$ gene have been deposited in GenBank under accession Nos. KJ997965 and KJ768338.

3. Results and discussion

3.1. Identification of the *bla*$_{\text{ADC68}}$ gene from carbapenem-resistant *A. baumannii* D015

Carbapenem-resistant *A. baumannii* D015 was resistant to piperacillin and all tested cephalosporins and carbapenems (Table 2). An ADC-type gene from *A. baumannii* D015 was detected. Sequence analysis revealed an 1152 bp open reading frame (ORF) that encoded a 383-amino-acid protein. This sequence differs from those of the previously reported ADC-type genes; following the recently developed uniform numerical system for this family of AmpC β-lactamases, we named this protein ADC-68. ADC-68 shared 34.2–43.5% sequence identity with other class C enzymes and 98% sequence identity with ADC-1. A detailed examination of the amino-acid sequences of ADC-68 compared with ADC-1 was then carried out based on amino-acid sequence alignment. Compared with ADC-1, ADC-68 has seven amino-acid substitutions (G77A, K128Q, S145P, T179I, P194A, G220D and R320G).

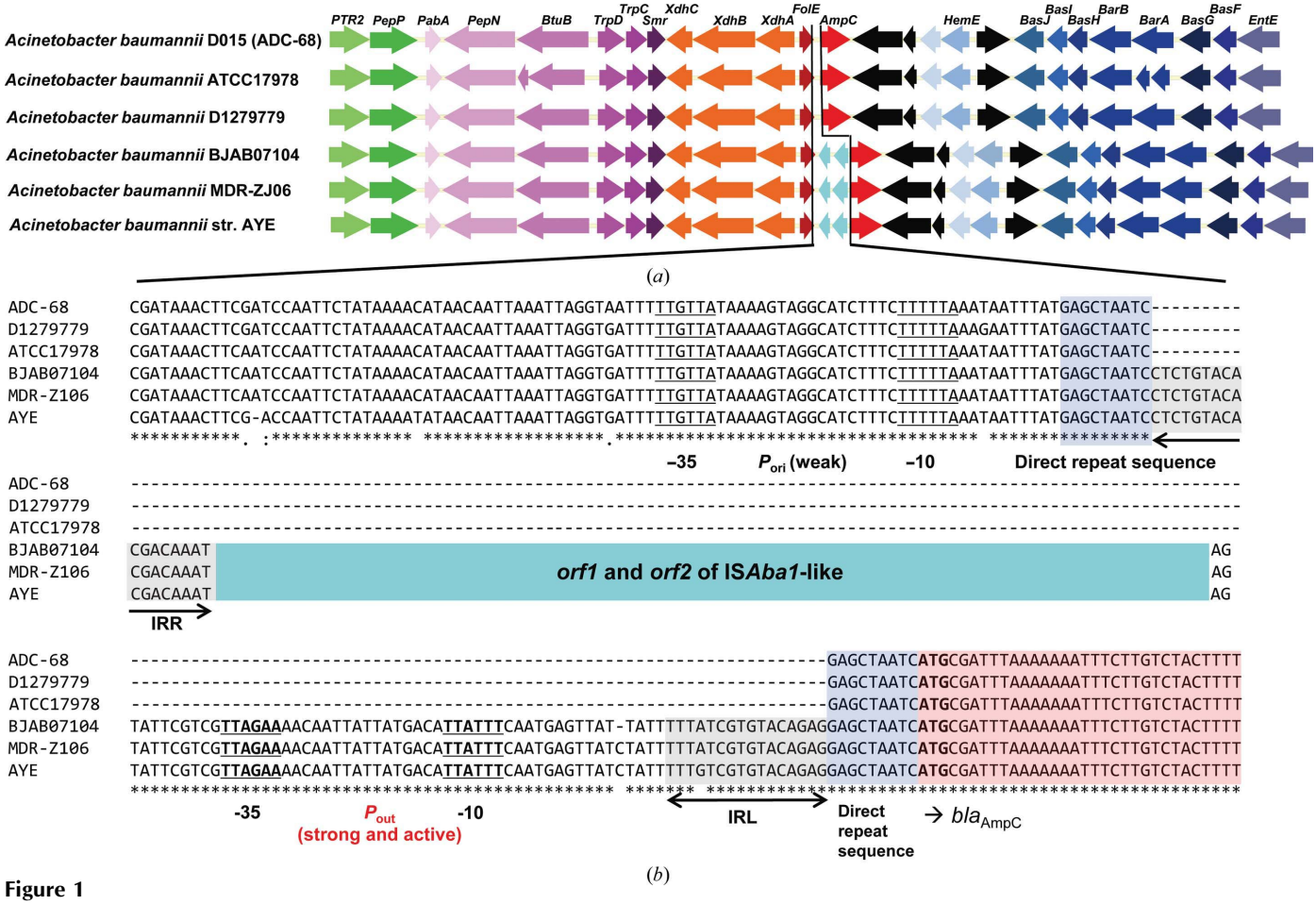

Figure 1
(*a*) Comparison of the genomic region surrounding the *bla*$_{\text{AmpC}}$ (*bla*$_{\text{ADC-68}}$) gene of *A. baumannii* D015 with those of *A. baumannii* ATCC 17978 (GenBank accession No. CP000521), *A. baumannii* D1279779 (accession No. CP003967), *A. baumannii* BJAB07104 (accession No. CP003846), *A. baumannii* MDR-ZJ06 (accession No. CP003500) and *A. baumannii* strain AYE (accession No. CU459141). (*b*) Multiple alignment analysis of the nucleotide sequences that are upstream of *bla*$_{\text{AmpC}}$ (a class C β-lactamase gene) in six *A. baumannii* strains. Direct repeat (DR) sequences are shown in blue, and the right and left inverted-repeat sequences (IRR and IRL, respectively) are in grey. Orf1 and orf2 (transposases) of IS*Aba1*-like elements are shown in cyan and *bla*$_{\text{AmpC}}$ is in red. The −35 and −10 motifs of the promoters are indicated. P_{out} is the promoter of *bla*$_{\text{AmpC}}$ provided by IS*Aba1*-like elements and P_{ori} is the putative host-cell promoter driving the expression of *bla*$_{\text{AmpC}}$ in the absence of IS*Aba1*-like elements.

Table 2
Minimum inhibitory concentrations (MICs) of β-lactams for a clinical isolate (*A. baumannii* D015), transformants harbouring $bla_{\text{ADC-1}}$ and $bla_{\text{ADC-68}}$ genes, host strains (*E. coli* TOP10 and *E. coli* JM83) and an MIC reference strain (*E. coli* ATCC 25922).

	MIC (mg l^{-1}) for organism				
β-Lactam	*E. coli* ATCC 25922	*E. coli* TOP10	*A. baumannii* D015 (ADC-68)	*E. coli* TOP10 (ADC-68)†	*E. coli* JM83 (ADC-1)/ *E. coli* JM83‡
Ampicillin	4	4	256	256	2048/2
Piperacillin	4	4	128	128	256/2
Piperacillin–tazobactam§	4	2	64	64	ND¶
Amoxicillin	8	4	256	256	ND
Amoxicillin–clavulanic acid (2:1)	8	4	256	256	ND
Cephalothin	8	4	>256	256	2048/4
Cefotaxime	0.06	0.06	32	32	64/0.03
Ceftazidime	0.5	0.5	16	16	256/0.125
Imipenem	0.25	0.5	8	8	ND
Meropenem	0.015	0.015	4	4	ND
Ertapenem	0.015	0.015	16	16	ND

† Transformant producing the ADC-68 β-lactamase of *A. baumannii* D015. ‡ The data for the transformant producing the ADC-1 β-lactamase and the host strain have been published previously (Bhattacharya *et al.*, 2014). § Inhibitor fixed at 4 µg ml^{-1}. ¶ Not determined.

To find the location of the $bla_{\text{ADC-68}}$ gene in *A. baumannii* D015, PFGE and Southern blot analysis were performed. Five DNA fragments were generated using the I-*Ceu*I fragment (Supplementary Fig. S1*a*). After the DNA fragments had been transferred onto a nylon membrane, five that were generated with the I-*Ceu*I fragment hybridized with a 16S rRNA-specific probe (Supplementary Fig. S1*b*), whereas probes specific for $bla_{\text{ADC-68}}$ were hybridized with two fragments (Supplementary Fig. S1*c*). From the draft genome sequence of *A. baumannii* D015, another bla_{AmpC} gene (GenBank accession No. KJ997965) that is homologous to $bla_{\text{ADC-68}}$ was found. In addition, probes specific for another bla_{AmpC} gene strongly hybridized with the upper band of the two fragments (Supplementary Fig. S1*d*). These results demonstrate that the $bla_{\text{ADC-68}}$ gene, which is responsible for β-lactam resistance, was located in the chromosome.

3.2. Genetic studies

To examine the region surrounding $bla_{\text{ADC-68}}$, we performed draft genome sequencing of *A. baumannii* D015. The final assembly contains 54 contigs (3926 coding DNA sequences, 4 088 373 bp, 39.01% G+C ratio) and 60 tRNA genes. The $bla_{\text{ADC-68}}$ gene was found in a 40 kb DNA fragment. The region surrounding ADC-68 is very similar to those in all of the genomic sequences of *A. baumannii* strains (Fig. 1*a*). *A. baumannii* D015 did not have insertion-sequence (IS) elements such as IS*Aba1* preceding the $bla_{\text{ADC-68}}$ gene; however, IS*Aba1*-like elements were located between the *folE* and bla_{AmpC} genes of three *A. baumannii* strains (Fig. 1). The original promoter sequences (P_{ori}) that drive bla_{AmpC} expression in the absence of any IS elements can be replaced by new promoter sequences (P_{out}) for the bla_{AmpC} gene (Fig. 1*b*). IS*Aba1* with terminal 16 bp inverted repeats (IRs), located next to a region of direct repeats (DRs) that is 9 bp upstream of the start codon of the bla_{AmpC} gene, has previously been reported (Héritier *et al.*, 2006). When transposition occurred between the *folE* and bla_{AmpC} genes, a duplicated 9 bp (DR) region of the target sequence was found (Héritier *et al.*, 2006). All *A. baumannii* strains also had a conserved a 9 bp (DR) upstream of the start codon of the bla_{AmpC} gene (Fig. 1*b*). ADC enzymes are non-inducible compared with other class C β-lactamases and confer resistance to penicillins and narrow-spectrum cephalosporins owing to their low expression levels (Hujer *et al.*, 2005; Bou & Martínez-Beltrán, 2000).

Since the acquisition of an IS element (predominantly IS*Aba1*) provides ADC genes with a strong promoter, these ADCs show much higher expression levels and can confer resistance to extended-spectrum cephalosporins such as cefotaxime and ceftazidime (Perez *et al.*, 2007). However, ADC-68 is capable of conferring resistance to extended-spectrum cephalosporins and carbapenems without ISs. We hypothesize that amino-acid mutations in ADC-68 could play an important role in conferring resistance to extended-spectrum cephalosporins and carbapenems.

3.3. Antimicrobial susceptibility testing

A. baumannii D015 was resistant to carbapenems as well as extended-spectrum cephalosporins. To verify whether the extended substrate spectrum of *A. baumannii* D015 is caused by ADC-68, the MICs of β-lactams for *E. coli* TOP10 producing ADC-68 were determined. The β-lactam pattern (resistance to all tested β-lactams, including carbapenems as well as extended-spectrum cephalosporins) of *E. coli* TOP10 producing ADC-68 was identical to that of *A. baumannii* D015 (Table 2). Unlike *E. coli* JM83 producing ADC-1, which is resistant to extended-spectrum cephalosporins (Bhattacharya *et al.*, 2014), the ADC-68-producing strain is resistant to carbapenems as well as extended-spectrum cephalosporins. This result indicates that ADC-68 from *A. baumannii* D015 possesses the properties of cESBLs and carbapenemases.

3.4. Biochemical properties

The purified ADC-68 was used for IEF analysis and kinetic measurements. IEF analysis identified a pI value of 9.4 for the purified ADC-68, which corresponds to those of the chromosomal cephalosporinases (ADC variants), which have highly alkaline isoelectric points (pI > 9.0). The IC_{50} values were >1000 µ*M* for clavulanic acid, 49.2 µ*M* for tazobactam and 260 µ*M* for sulbactam. Among the three clinically used inhibitors, tazobactam and sulbactam were weak inhibitors, whereas clavulanic acid did not affect the enzyme activity. This result correlated with little (or no) decrease in the MICs of penicillins in the case of β-lactam inhibitor combinations (Table 2).

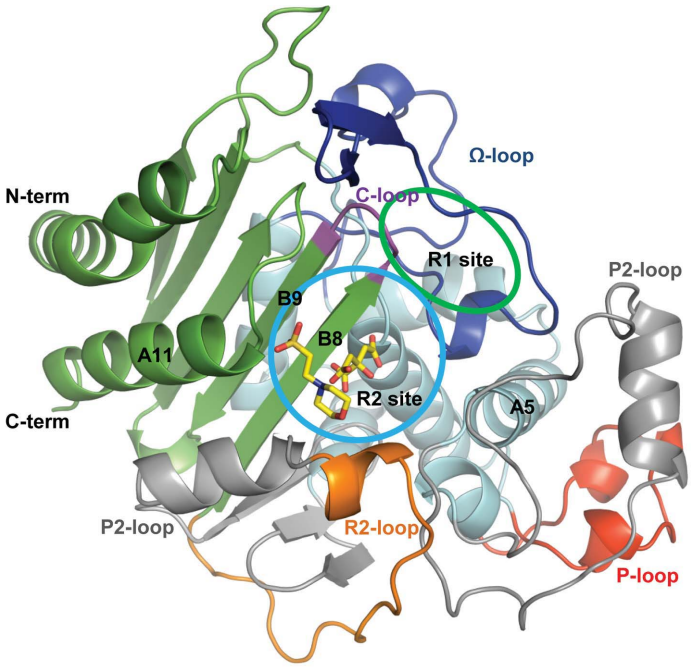

(*a*)

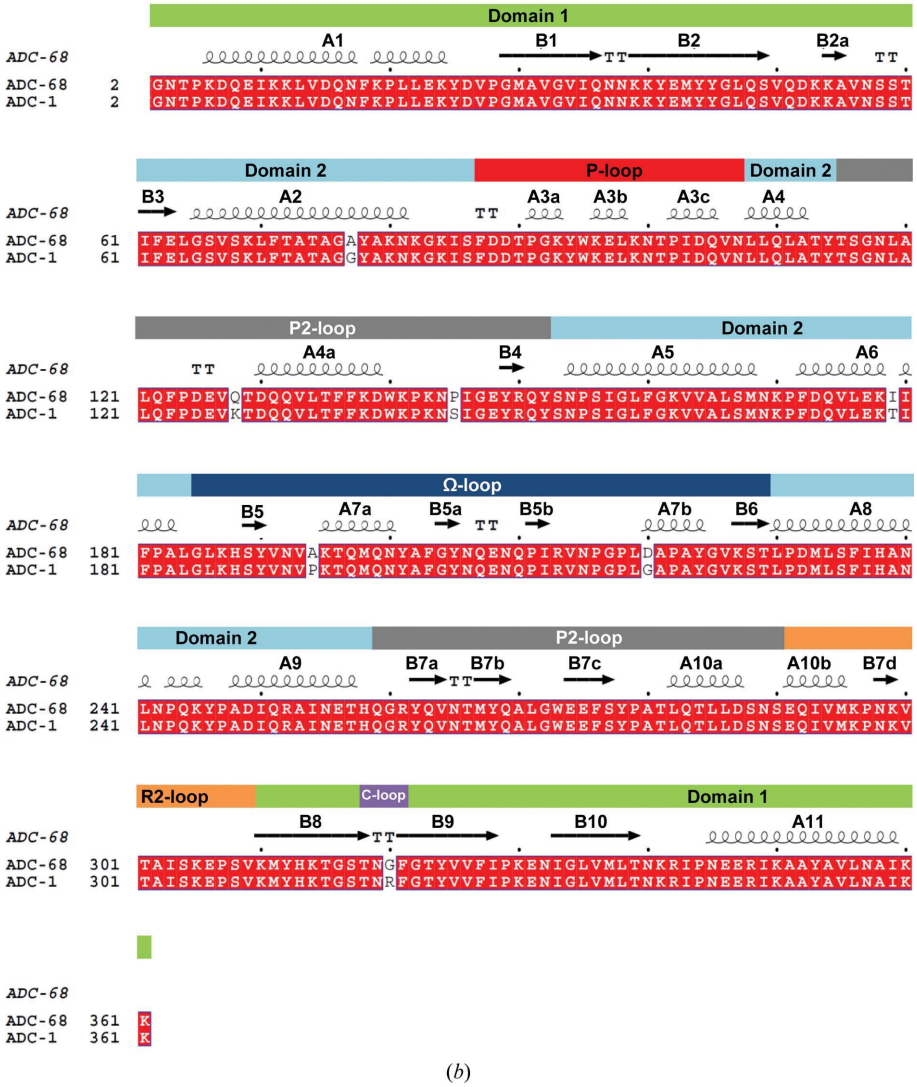

(*b*)

Kinetic analysis of ADC-68 revealed that this enzyme has a broad substrate profile that includes carbapenems (Table 3). Kinetic data revealed that the catalytic efficiencies of ADC-68 for all tested β-lactams except for carbapenems were similar to those of the cESBL ADC-1 (Table 3). The catalytic efficiencies of ADC-68 for cefotaxime and ceftazidime are similar to those of ADC-1, which indicates that ADC-68 is a cESBL.

The carbapenemase activities of three representative plasmid-borne class C β-lactamases (CMY-2, ACT-1 and CMY-10) have been reported (Mammeri *et al.*, 2010; Kim *et al.*, 2006). Unlike other ADC-type enzymes, ADC-68 showed hydrolytic activity against imipenem, meropenem and ertapenem. In the case of ADC-1, a previous report (Bou & Martínez-Beltrán, 2000) revealed that carbapenems were not hydrolyzed at detectable levels. The catalytic efficiency of ADC-68 for imipenem (0.17 μM^{-1} s^{-1}) was fourfold and 24-fold higher than those of CMY-2 and ACT-1 (0.04 and 0.007 μM^{-1} s^{-1}, respectively), but was similar to that of CMY-10 (a plasmid-mediated cESBL and class C carbapenemase) from *E. aerogenes*, KPC-1 (a class A carbapenemase) from *Klebsiella pneumoniae*, CAU-1 (a class B carbapenemase) from *Caulobacter crescentus*, NDM-1 (a class B carbapenemase) from *Klebsiella pneumonia* and OXA-48 (a class D carbapenemase) from *K. pneumonia* (the catalytic efficiencies were 0.14, 0.15, 0.2, 0.21 and 0.145 μM^{-1} s^{-1}, respectively; Mammeri *et al.*, 2010; Kim *et al.*, 2006; Yong *et al.*, 2009; Poirel *et al.*, 2004; Docquier *et al.*, 2002; Yigit *et al.*,

Figure 2
Overall structure of ADC-68 from *A. baumannii*. (*a*) Ribbon diagram showing the overall fold of the ADC-68 structure. Domain 1 (green), domain 2 (cyan) and the P-loop (red), P2-loop (dark grey), Ω-loop (blue), R2-loop (orange) and C-loop (magenta) are indicated. 2-(*N*-Morpholino) ethanesulfonic acid (MES) and citrate are represented as sticks in yellow. The R1 and R2 subsites are indicated as green and cyan circles, respectively. (*b*) A structure-based sequence alignment of ADC-68 with ADC-1. Conserved residues are shown as white letters in red boxes. Conservative substitutions are placed in white boxes.

Table 3
Comparison of the kinetic parameters of the ADC-68 β-lactamase with those of ADC-1 for various β-lactams.

	ADC-68			ADC-1†		
Substrate	k_{cat} (s^{-1})	K_m (μM)	k_{cat}/K_m ($\mu M^{-1}\,s^{-1}$)	k_{cat} (s^{-1})	K_m (μM)	k_{cat}/K_m ($\mu M^{-1}\,s^{-1}$)
Benzylpenicillin	85.4 ± 0.4	23.5 ± 0.2	3.63 ± 0.03	10.26 ± 0.27	5.1 ± 0.3	2.0 ± 0.35
Ampicillin	7.1 ± 0.5	20.3 ± 0.21	0.35 ± 0.02	4.8 ± 0.18	32.0 ± 7	0.15 ± 0.03
Piperacillin	9.3 ± 0.4	19.2 ± 0.5	0.48 ± 0.01	3.1 ± 0.14	6.4 ± 1.4	0.48 ± 0.1
Cephalothin	65.8 ± 1.5	21.5 ± 0.2	3.06 ± 0.03	147.0 ± 9.0	74.0 ± 8.6	2.0 ± 0.2
Cefotaxime	18.5 ± 0.5	117.5 ± 1.3	0.16 ± 0.02	0.16 ± 0.01	0.5 ± 0.04	0.32 ± 0.032
Ceftazidime	1.66 ± 0.06	147.7 ± 1.2	0.01 ± 0.003	0.7 ± 0.02	16.0 ± 1.7	0.044 ± 0.005
Imipenem	0.14 ± 0.002	0.83 ± 0.004‡	0.17 ± 0.001	ND§	ND	ND
Meropenem	0.15 ± 0.001	2.03 ± 0.002‡	0.07 ± 0.001	ND	ND	ND
Ertapenem	0.12 ± 0.001	9.87 ± 0.003‡	0.01 ± 0.003	ND	ND	ND

† The data for ADC-1 have been published previously (Bhattacharya *et al.*, 2014). ‡ Determined K_i values. § Not determined because ADC-1 could not hydrolyze carbapenems as previously reported (Bou & Martínez-Beltrán, 2000).

2001). These kinetic data indicate carbapenem-hydrolyzing activity and are therefore consistent with the determined MICs. Taken together, we concluded that ADC-68 has cESBL and carbapenemase properties.

3.5. Overall structure of ADC-68 β-lactamase

To verify the mechanism by which ADC-68 expands its substrate spectrum to extended-spectrum cephalosporins and carbapenems, we determined the crystal structure of ADC-68. ADC-68 from *A. baumannii* D015 was crystallized in the orthorhombic space group $P2_12_12_1$. The crystal structure of ADC-68 was determined by molecular replacement using CMY-10 (Kim *et al.*, 2006) as a search model and was refined at 1.8 Å resolution (Table 1). There were two ADC-68 molecules in the asymmetric unit, and each ADC-68 molecule was composed of 361 residues (residues 5–361 are visible in the electron-density map). The protein structure was refined with r.m.s.d.s of 0.020 Å and 1.982° for the bond lengths and angles, respectively. A Ramachandran plot that was calculated with *PROCHECK* (Laskowski *et al.*, 1993) revealed that 99.6% of the residues are in the most favoured and additionally allowed regions. The overall structure of ADC-68 was conserved in other class C β-lactamases and consists of two main domains [domain 1 (Pro5–Thr60 and Lys310–Lys361) and domain 2 (Ile61–Val309)] and the P-loop (Phe87–Asn107), P2-loop (Thr115–Tyr152 and Glu259–Ser290), Ω-loop (Gly185–Thr229), R2-loop (Glu291–Val309) and C-loop (Thr318–Phe321) (Fig. 2).

The active site of β-lactamase was divided into R1 and R2 subsites based on the corresponding binding sites of the R_1 and R_2 side chains of β-lactams. The R1 subsite of the β-lactamase, the upper pocket of the total substrate-binding pocket, is surrounded by the Ω-loop, A5, the P2-loop and the loop (Thr318–Phe321) between B8 and B9, which we named the C-loop because of the structural possibility of the

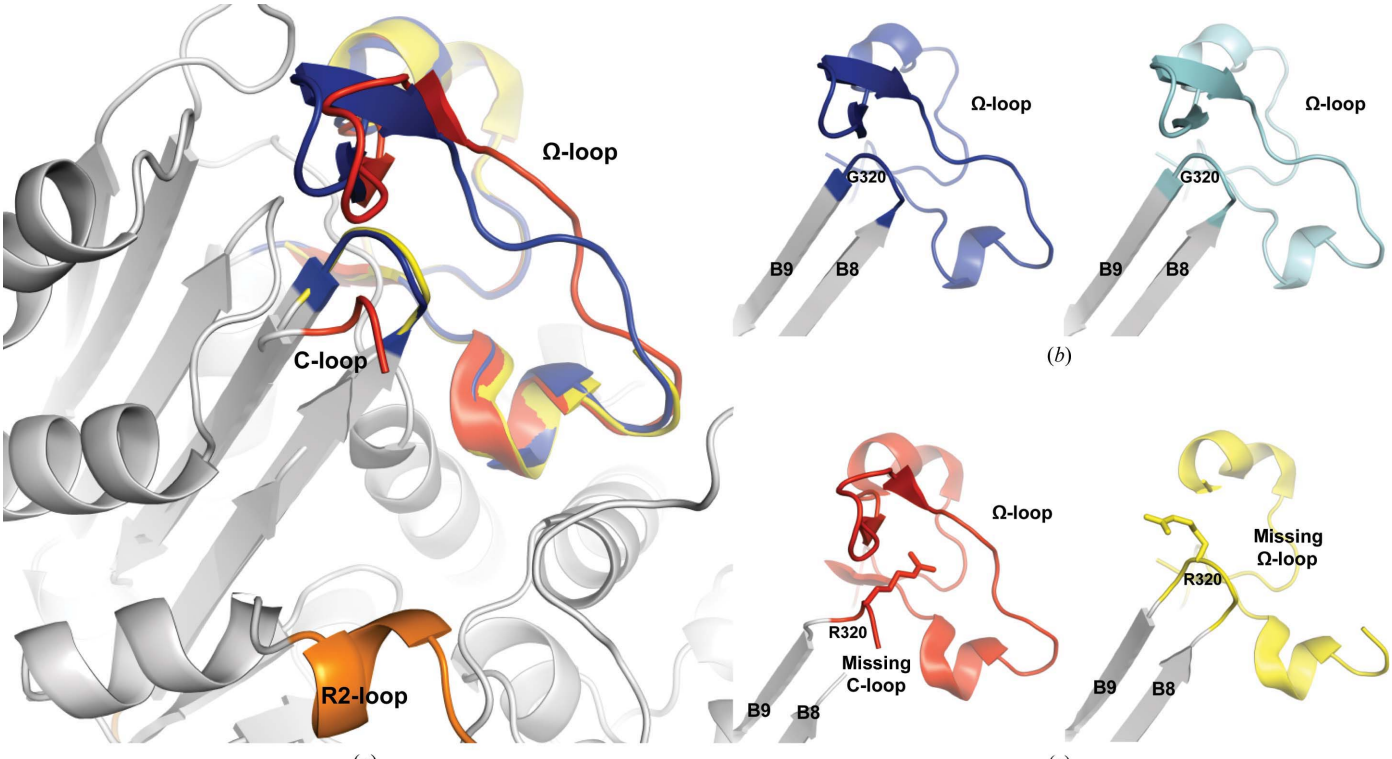

Figure 3
Structural comparison between ADC-68 and ADC-1. (*a*) Superposition of ADC-68 molecule *A* (blue), ADC-1 molecule *A* (red) and ADC-1 molecule *B* (yellow). The Ω-loop and C-loop structures are represented as a ribbon diagram. (*b*) Superposition of ADC-68 molecule *A* (blue) and ADC-68 molecule *B* (cyan). (*c*) Superposition of ADC-1 molecule *A* (red) and ADC-1 molecule *B* (yellow).

importance of this region in acquiring carbapenemase activity. The R2 subsite, which is the lower pocket of the total substrate-binding pocket, is formed by the C-loop, including B8, the P2-loop, A11 and the R2-loop. In the ADC-68 crystal structure, two molecules of MES and citrate from the crystallization solution were bound in the R2 subsite.

3.6. Structural comparison between the ADC-68 and ADC-1 β-lactamases

The ADC-68 (a carbapenemase) structure was compared with that of ADC-1 (a non-carbapenemase; PDB entry 4net; 98% sequence identity), which is a cESBL from *A. baumannii* (Fig. 2*b*; Bhattacharya *et al.*, 2014). Among the 361 amino acids of ADC-68, seven amino acids differed from those in ADC-1. One of these seven (Gly320 in ADC-68) is located in the C-loop, which is important for the carbapenemase characteristics, and two (Ala194 and Asp220 in ADC-68) are found in the Ω-loop (Gly185–Thr229).

Although the overall structures of ADC-68 and ADC-1 were conserved, noticeable structural differences were found in the Ω-loop and the C-loop (Fig. 3*a*). In particular, the two residues Gly320 and Asp220 in ADC-68 contributed to the major structural differences between ADC-68 and ADC-1. In both the ADC-68 and the ADC-1 crystal structures two molecules were present in the asymmetric unit. In ADC-68, the Ω-loop and C-loop structures of the two molecules exhibit the same conformation (Fig. 3*b*). However, ADC-1 had different conformations in the two molecules. The structure of ADC-1 molecule *A* did not show the residues Ser317 and Thr318 in B8 and the C-loop, respectively, and the residues Asn319 and Arg320 in the C-loop bulged into the central R2 subsite (Fig. 3*c*). In contrast, the structure of ADC-1 molecule *B* lacked the central part of the Ω-loop (Phe203–Pro216) and had an intact C-loop.

The C-loop is located just beneath the central part of the Ω-loop (Fig. 3*c*). Accordingly, the conformation of the C-loop is directly related to that of the adjacent Ω-loop. Compared with Arg320 in ADC-1, ADC-68 has the much smaller Gly320 residue in the C-loop. The bulkier Arg320 residue of the C-loop in the ADC-1 structure simultaneously interfered with the stable formation of both the C-loop and the central Ω-loop

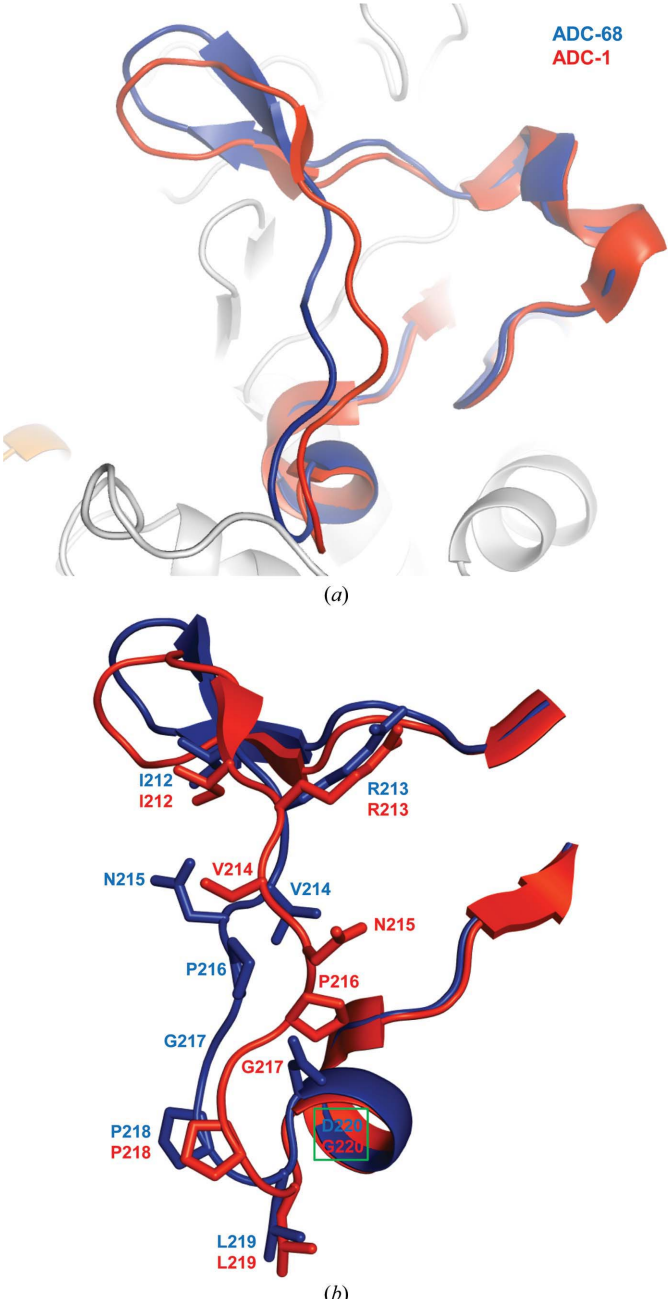

Figure 4
Structural difference between ADC-68 and ADC-1 in the Ω-loop. (*a*) The Ω-loops are represented as a ribbon diagram: ADC-68, blue; ADC-1, red. (*b*) The Ω-loops are represented as sticks: ADC-68, blue; ADC-1, red.

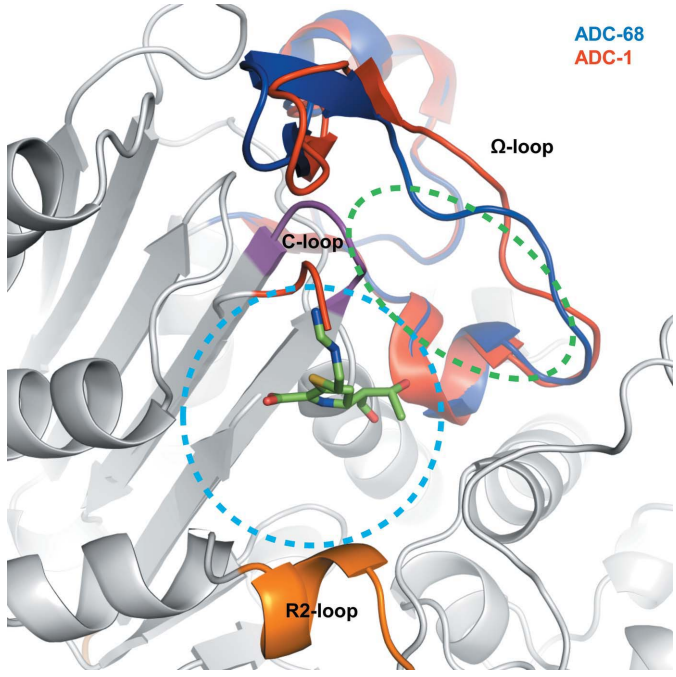

Figure 5
Superimposed complex of imipenem with ADC-68 and ADC-1. An AmpC complex with imipenem was superposed with ADC-1 and ADC-68. ADC-68 and ADC-1 are represented as blue and red ribbon diagrams, respectively. Imipenem is represented as green sticks. The R1 and R2 subsites are indicated as green and cyan dotted circles, respectively.

because of steric hindrance. When the central Ω-loop was activated in ADC-1 molecule *A* it pushed the C-loop into the R2 subsite, also disrupting part of the B8 strand (Fig. 3*c*). In ADC-1 molecule *B*, in which the complete C-loop was formed, the central Ω-loop was also disordered because of steric hindrance. In the ADC-68 crystal structure both molecules had an intact Ω-loop and C-loop, and the complete C-loop remained in line with B8 and B9 and provided a wide-open conformation of the R2 subsite compared with the bulged-in C-loop of ADC-1.

Another structural difference in the Ω-loop was caused by the bulkier residue Asp220 in ADC-68 compared with Gly220 in ADC-1, which shifted the right side of the Ω-loop (Ile212–Leu219) towards the centre of the R1 subsite; the C^{α} atom of the Asn215 residue shifted inwards by 4.3 Å and it rotated almost 110° towards the R1 subsite (Fig. 4). In both the ADC-68 and ADC-1 structures this part of the Ω-loop was not involved in crystal packing.

3.7. Structural basis for the extended substrate spectrum of ADC-68 β-lactamase

Since the kinetic parameters of ADC-68 for all tested β-lactams except for the carbapenems were similar to those of ADC-1, we superimposed the carbapenem-bound AmpC structure (PDB entry 1ll5; Beadle & Shoichet, 2002) with ADC-68 (r.m.s.d. of 1.18 Å with 330 C^{α} atoms aligned) and ADC-1 with the bulged-in C-loop (r.m.s.d. of 1.30 Å with 327 C^{α} atoms aligned).

The R_2 side chain of imipenem (a carbapenem) was exactly superimposed on the bulged-in C-loop of ADC-1, and imipenem could not be accommodated in the R2 subsite of ADC-1 (Fig. 5). In ADC-68 no steric hindrance was observed (Figs. 5 and 7*d*). Similar to imipenem, both meropenem and ertapenem (carbapenems) have bulkier R_2 side chains. We speculate that the stable open conformation of the R2 subsite of ADC-68 helped to bind the carbapenems.

Crystallographic and biochemical research on the ADC-1 and CMY-10 enzymes has demonstrated that their extended substrate spectrum involves alterations of the R2-loop connecting strands B7d and B8 (Bhattacharya *et al.*, 2014; Kim *et al.*, 2006). ADC-68 also has a three-amino-acid deletion in the R2-loop as in ADC-1 and CMY-10, which causes a widening of the R2 binding pocket by forming a wide-open conformation of the R2-loop to bind to the bulky R_2 substituents of extended-spectrum cephalosporins (Fig. 6*a*). Compared with CMY-10 and ADC-1, the 3_{10}-helix of the R2-loop in ADC-68 shifted towards the outside of the protein by 0.8 and 0.4 Å, respectively, thus forming slightly wider R2 subsites than in ADC-1 and CMY-10 (Fig. 6*b*).

Another difference between the ADC-68 and ADC-1 structures is that the right side of the Ω-loop was moved into the central R1 subsite in ADC-68. However, there was still enough room to accommodate the R_1 chains of cefotaxime and ceftazidime in ADC-68. The closest distances between the right-side Ω-loop of ADC-68 and the R_1 side chains of cefotaxime and ceftazidime were 3.3 Å to a side chain (4.5 Å to the C^{α} atom), and no steric hindrance was observed (Supplementary Fig. S2).

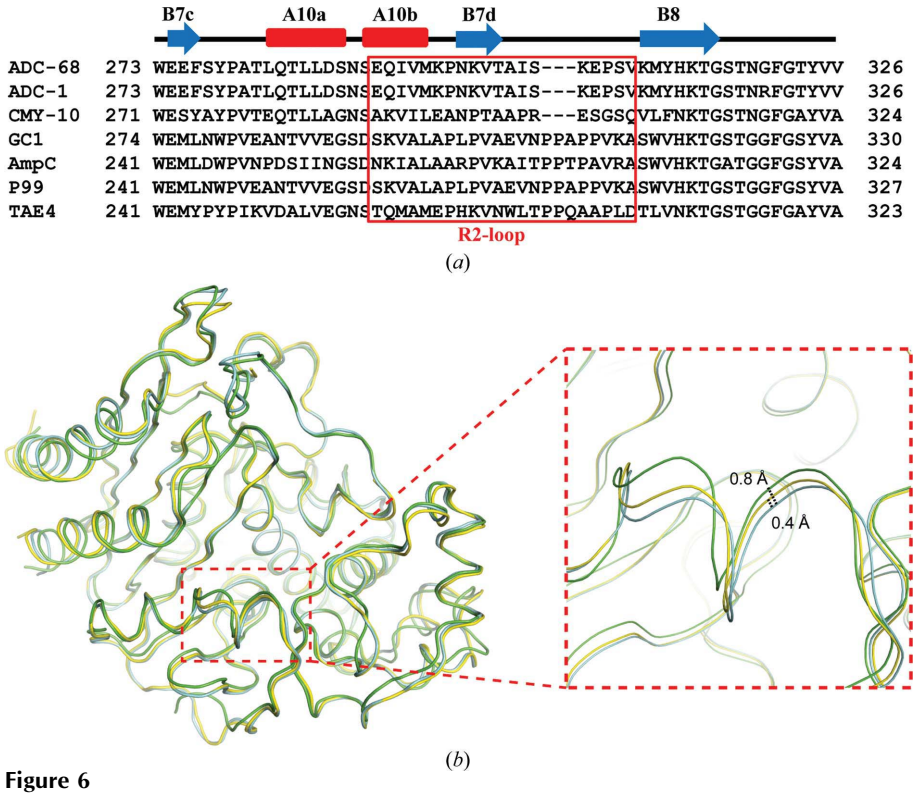

Figure 6
(*a*) Structure-based sequence alignment of the R2-loop region of ADC-68 with class C β-lactamases: ADC-1 (PDB entry 4net) from *A. baumannii*, CMY-10 (PDB entry 1zkj) from *E. aerogenes*, GC1 (PDB entry 1gce) from *E. cloacae*, AmpC (PDB entry 2bls) from *E. coli*, P99 (PDB entry 1xx2) from *E. aerogenes* and TAE4 (PDB entry 2qz6) from *P. fluorescens*. The R2-loop residues are indicated by and shown in the red box. (*b*) Superposition of ADC-68 (cyan ribbon), ADC-1 (yellow ribbon) and CMY-10 (green ribbon). The red dashed square shows the R2-loop region. The distance of the R2-loop between ADC-68 and ADC-1 (0.4 Å) as well as CMY-10 (0.8 Å) are shown by black dashed lines.

3.8. Bound conformations of cephalosporins and imipenem in AmpC structures

When we superimposed AmpC (class C β-lactamase from *E. coli*) structures in complex with cephalosporins such as cephalothin (PDB entry 1kvm; r.m.s.d. of 1.22 Å with ADC-68 for 338 aligned C^{α} atoms; Beadle *et al.*, 2002), cefotaxime (PDB entry 3ixh; r.m.s.d. of 1.24 Å for 339 aligned C^{α} atoms; Thomas *et al.*, 2010) and ceftazidime (PDB entry 1iel; r.m.s.d. of 1.25 Å for 339 aligned C^{α} atoms; Powers *et al.*, 2001), and with a carbapenem such as

imipenem (PDB entry 1ll5; r.m.s.d. of 1.18 Å with 330 aligned C^{α} atoms; Beadle & Shoichet, 2002), the cephalosporins and imipenem had different binding conformations.

Since the AmpC crystal structures used were the acyl-enzyme complexes with the cephalosporins, the β-lactam ring of the drug is opened and covalently attached to the catalytic serine. The resulting cephalosporin structures were bent into a 'U' form to bring the R_1 and R_2 side chains of the cephalosporins closer in the three-dimensional structure (Figs. 7*a*, 7*b* and 7*c*). Accordingly, the R_1 side chains of the cephalosporins were positioned close to between the C-loop and Ω-loop. The closest distances between the C3 atom of the dihydrothiazine ring in the cephalosporin core structure and the terminal parts of various R_1 groups were 3.8–6.9 Å, averaging at only 4.5 Å in cephalothin, cefotaxime and ceftazidime (Thomas *et al.*, 2010; Beadle *et al.*, 2002; Powers *et al.*, 2001). Except for cephalothin (a narrow-spectrum cephalosporin), the average distance was as small as 3.9 Å. The R_1 groups of the extended-spectrum cephalosporins of cefotaxime and ceftazidime have an aminothiazole ring and oxyimino group in common, and their relative binding positions in the complex structures were reversed because of the different size of the oxyimino-attached groups (Figs. 7*b* and 7*c*).

The terminal ring structures attached to the R_1 side chain of cephalosporins were positioned in the R1 subsite, particularly between the C-loop and the central Ω-loop. The other side (R_2 side) of cephalosporins was bound to the R2 subsite, which was surrounded by the C-loop and the R2-loop at the upper and lower boundaries. The C-loop is located just next to the catalytic Ser66 residue in helix2 and at the border between the

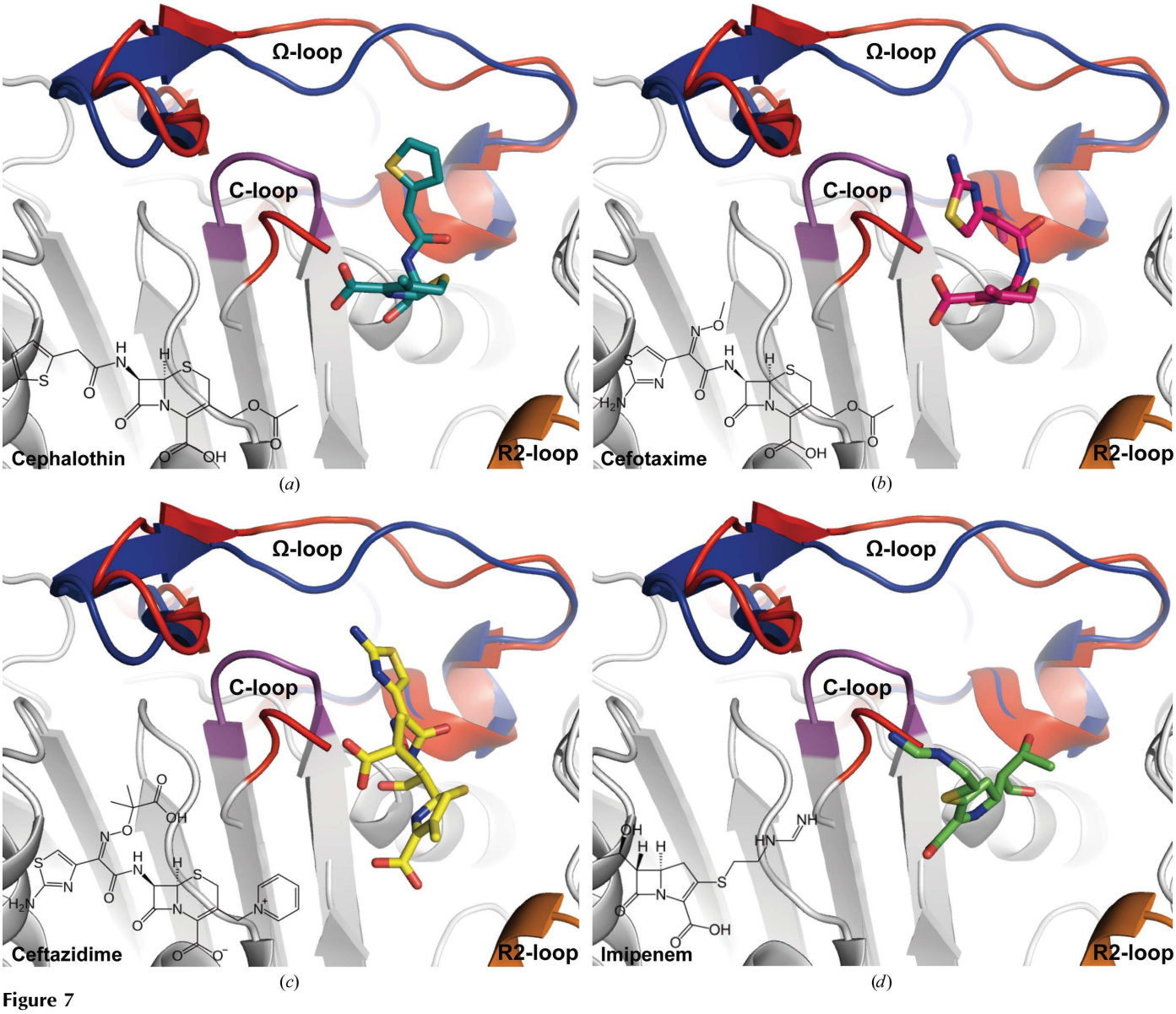

Figure 7
The superimposed complex structures of cephalosporins and imipenem with ADC-68 and ADC-1. The Ω-loops of ADC-68 and ADC-1 are represented as blue and red ribbon diagrams, respectively. The C-loops of ADC-68 and ADC-1 are represented as magenta and red ribbon diagrams, respectively. The R2-loop showing no conformational difference between ADC-68 and ADC-1 is represented as an orange ribbon diagram. The ligands are represented as sticks. (*a*) Cephalothin, (*b*) cefotaxime, (*c*) ceftazidime and (*d*) imipenem.

R1 and R2 subsites. Accordingly, the C-loop conformation could directly affect the active-site geometry of both the R1 and the R2 subsites simultaneously and is important for the extended substrate spectrum of β-lactamases.

The imipenem core structure was more linear than the rolled-up 'U' form of cephalosporins. Similar to the cephalosporin-bound structures, the imipenem β-lactam ring was also cleaved and the carbonyl group of the cleaved β-lactam ring was linked to the catalytic serine residue. The shorter chain of the α-hydroxyethyl group was at the R_1 position of the core β-lactam structure. The longer iminomethylamino group containing a chain at the R_2 position was bound at the R2 subsite (Fig. 7*d*). The shorter R_1 part of imipenem occupied the R1 subsite close to the right side of the Ω-loop and did not interact with the C-loop and the central Ω-loop. The longer R_2 part was mostly bound in the R2 subsite, which was close to the C-loop position. Accordingly, carbapenems could be more sensitive to R2 subsite geometry than cephalosporins.

4. Conclusion

We found a novel ADC-68 β-lactamase from *A. baumannii* D015 that is resistant to carbapenems as well as extended-spectrum cephalosporins. ADC-68 is the first cESBL and carbapenemase among the class C β-lactamases that is encoded by a chromosomal gene. Although three plasmid-borne class C β-lactamases (CMY-2, ACT-1 and CMY-10) showed carbapenemase activity (Mammeri *et al.*, 2010; Kim *et al.*, 2006), ADC-type enzymes (except for ADC-68) did not show hydrolytic activity against carbapenems such as imipenem, meropenem and ertapenem. These kinetic data are consistent with the determined MICs that revealed the presence of carbapenem resistance.

The ADC-68 structure showed a stable, wide-open conformation in the R2 subsite *via* a straight C-loop with B8 and B9 as well as an R2-loop opening because of its three-amino-acid deletion, which is important for both the cESBL and the carbapenemase activities. The ADC-1 structure revealed an unstable C-loop conformation, which could inhibit the binding of imipenem or other carbapenems more than cephalosporins.

This work was supported by research grants from the National Research Laboratory Program through the National Research Foundation of Korea (NRF) funded by the Ministry of Science, ICT and Future Planning (No. 2011-0027928), the Marine and Extreme Genome Research Center Program funded by the Ministry of Oceans and Fisheries, Republic of Korea and the Introduced Innovative R&D Team Leadership of Guangdong Province, People's Republic of China.

References

Afzal-Shah, M. & Livermore, D. M. (1998). *J. Antimicrob. Chemother.* **41**, 576–577.
Barton, B. M., Harding, G. P. & Zuccarelli, A. J. (1995). *Anal. Biochem.* **226**, 235–240.
Beadle, B. M. & Shoichet, B. K. (2002). *Antimicrob. Agents Chemother.* **46**, 3978–3980.
Beadle, B. M., Trehan, I., Focia, P. J. & Shoichet, B. K. (2002). *Structure*, **10**, 413–424.
Beceiro, A., Dominguez, L., Ribera, A., Vila, J., Molina, F., Villanueva, R., Eiros, J. M. & Bou, G. (2004). *Antimicrob. Agents Chemother.* **48**, 1374–1378.
Bergogne-Bérézin, E. & Towner, K. J. (1996). *Clin. Microbiol. Rev.* **9**, 148–165.
Bhattacharya, M., Toth, M., Antunes, N. T., Smith, C. A. & Vakulenko, S. B. (2014). *Acta Cryst.* D**70**, 760–771.
Bou, G. & Martínez-Beltrán, J. (2000). *Antimicrob. Agents Chemother.* **44**, 428–432.
Bradford, P. A., Urban, C., Mariano, N., Projan, S. J., Rahal, J. J. & Bush, K. (1997). *Antimicrob. Agents Chemother.* **41**, 563–569.
Clinical and Laboratory Standards Institute (2014). *M100-S24: Performance Standards for Antimicrobial Susceptibility Testing; Twenty-fourth Informational Supplement*. Wayne: Clinical and Laboratory Standards Institute.
Coelho, J., Woodford, N., Turton, J. & Livermore, D. M. (2004). *J. Hosp. Infect.* **58**, 167–169.
Crichlow, G. V., Kuzin, A. P., Nukaga, M., Mayama, K., Sawai, T. & Knox, J. R. (1999). *Biochemistry*, **38**, 10256–10261.
DeLano, W. L. (2002). *PyMOL*. http://www.pymol.org.
Delcher, A. L., Bratke, K. A., Powers, E. C. & Salzberg, S. L. (2007). *Bioinformatics*, **23**, 673–679.
De Meester, F., Joris, B., Reckinger, G., Bellefroid-Bourguignon, C., Frère, J.-M. & Waley, S. G. (1987). *Biochem. Pharmacol.* **36**, 2393–2403.
Disz, T., Akhter, S., Cuevas, D., Olson, R., Overbeek, R., Vonstein, V., Stevens, R. & Edwards, R. A. (2010). *BMC Bioinformatics*, **11**, 319.
Docquier, J.-D., Pantanella, F., Giuliani, F., Thaller, M. C., Amicosante, G., Galleni, M., Frère, J.-M., Bush, K. & Rossolini, G. M. (2002). *Antimicrob. Agents Chemother.* **46**, 1823–1830.
Emsley, P., Lohkamp, B., Scott, W. G. & Cowtan, K. (2010). *Acta Cryst.* D**66**, 486–501.
Galleni, M., Franceschini, N., Quinting, B., Fattorini, L., Orefici, G., Oratore, A., Frère, J.-M. & Amicosante, G. (1994). *Antimicrob. Agents Chemother.* **38**, 1608–1614.
Galleni, M. & Frère, J.-M. (1988). *Biochem. J.* **255**, 119–122.
Héritier, C., Poirel, L. & Nordmann, P. (2006). *Clin. Microbiol. Infect.* **12**, 123–130.
Hujer, K. M., Hamza, N. S., Hujer, A. M., Perez, F., Helfand, M. S., Bethel, C. R., Thomson, J. M., Anderson, V. E., Barlow, M., Rice, L. B., Tenover, F. C. & Bonomo, R. A. (2005). *Antimicrob. Agents Chemother.* **49**, 2941–2948.
Kim, J. Y., Jung, H. I., An, Y. J., Lee, J. H., Kim, S. J., Jeong, S. H., Lee, K. J., Suh, P.-G., Lee, H.-S., Lee, S. H. & Cha, S.-S. (2006). *Mol. Microbiol.* **60**, 907–916.
Kuzmic, P. (1996). *Anal. Biochem.* **237**, 260–273.
Laskowski, R. A., MacArthur, M. W., Moss, D. S. & Thornton, J. M. (1993). *J. Appl. Cryst.* **26**, 283–291.
Lee, J. H., Bae, I. K. & Lee, S. H. (2012). *Med. Res. Rev.* **32**, 216–232.
Lee, J. H., Jeong, S. H., Cha, S.-S. & Lee, S. H. (2009). *PLoS Pathog.* **5**, e1000221.
Lee, J. H. & Lee, S. H. (2006). *Res. J. Microbiol.* **1**, 1–22.
Lee, K., Yong, D., Choi, Y. S., Yum, J. H., Kim, J. M., Woodford, N., Livermore, D. M. & Chong, Y. (2007). *Int. J. Antimicrob. Agents*, **29**, 201–206.
Liu, S.-L., Hessel, A. & Sanderson, K. E. (1993). *Proc. Natl Acad. Sci. USA*, **90**, 6874–6878.
Mammeri, H., Guillon, H., Eb, F. & Nordmann, P. (2010). *Antimicrob. Agents Chemother.* **54**, 4556–4560.
Murshudov, G. N., Skubák, P., Lebedev, A. A., Pannu, N. S., Steiner, R. A., Nicholls, R. A., Winn, M. D., Long, F. & Vagin, A. A. (2011). *Acta Cryst.* D**67**, 355–367.
Nukaga, M., Haruta, S., Tanimoto, K., Kogure, K., Taniguchi, K., Tamaki, M. & Sawai, T. (1995). *J. Biol. Chem.* **270**, 5729–5735.
Otwinowski, Z. & Minor, W. (1997). *Methods Enzymol.* **276**, 307–326.

Paterson, D. L. & Bonomo, R. A. (2005). *Clin. Microbiol. Rev.* **18**, 657–686.
Perez, F., Hujer, A. M., Hujer, K. M., Decker, B. K., Rather, P. N. & Bonomo, R. A. (2007). *Antimicrob. Agents Chemother.* **51**, 3471–3484.
Poirel, L., Héritier, C., Tolün, V. & Nordmann, P. (2004). *Antimicrob. Agents Chemother.* **48**, 15–22.
Poirel, L. & Nordmann, P. (2006). *Clin. Microbiol. Infect.* **12**, 826–836.
Powers, R. A., Caselli, E., Focia, P. J., Prati, F. & Shoichet, B. K. (2001). *Biochemistry*, **40**, 9207–9214.
Queenan, A. M. & Bush, K. (2007). *Clin. Microbiol. Rev.* **20**, 440–458.
Richet, H. M., Mohammed, J., McDonald, L. C. & Jarvis, W. R. (2001). *Emerg. Infect. Dis.* **7**, 319–322.
Rodríguez-Martínez, J. M., Nordmann, P., Ronco, E. & Poirel, L. (2010). *Antimicrob. Agents Chemother.* **54**, 3484–3488.
Tatusov, R. L., Koonin, E. V. & Lipman, D. J. (1997). *Science*, **278**, 631–637.
Thomas, V. L., McReynolds, A. C. & Shoichet, B. K. (2010). *J. Mol. Biol.* **396**, 47–59.
Thomson, K. S. (2010). *J. Clin. Microbiol.* **48**, 1019–1025.
Tian, G.-B., Adams-Haduch, J. M., Taracila, M., Bonomo, R. A., Wang, H.-N. & Doi, Y. (2011). *Antimicrob. Agents Chemother.* **55**, 4922–4925.
Vagin, A. & Teplyakov, A. (2010). *Acta Cryst.* D**66**, 22–25.
Walsh, T. R., Gamblin, S., Emery, D. C., MacGowan, A. P. & Bennett, P. M. (1996). *J. Antimicrob. Chemother.* **37**, 423–431.
Yakupogullari, Y., Poirel, L., Bernabeu, S., Kizirgil, A. & Nordmann, P. (2008). *J. Antimicrob. Chemother.* **61**, 221–222.
Yigit, H., Queenan, A. M., Anderson, G. J., Domenech-Sanchez, A., Biddle, J. W., Steward, C. D., Alberti, S., Bush, K. & Tenover, F. C. (2001). *Antimicrob. Agents Chemother.* **45**, 1151–1161.
Yong, D., Toleman, M. A., Giske, C. G., Cho, H. S., Sundman, K., Lee, K. & Walsh, T. R. (2009). *Antimicrob. Agents Chemother.* **53**, 5046–5054.